

Ions at the Surface of a Room-Temperature Ionic Liquid

Cherry S. Santos, Selimar Rivera-Rubero, Sergey Dibrov, and Steven Baldelli*

Department of Chemistry, University of Houston, Houston, Texas 77204

Received: August 15, 2006; In Final Form: March 9, 2007

The orientation and interfacial location of both the cation and anion of the ionic liquids 1-butyl-3-methylimidazolium methyl sulfate and 1-butyl-3-methylimidazolium methanesulfonate have been determined by sum-frequency generation vibrational spectroscopy and X-ray crystallography. The results indicate that both the cation and anion occupy the first layer at the gas–liquid interface. Further, the methyl groups of the cation and anion are directed away from the liquid phase into the gas phase.

Introduction

Understanding the interfacial behavior of room-temperature ionic liquids at different interfaces such as solid–liquid, liquid–liquid, and air–liquid, is significant for industrial catalytic reactions and electrochemical processes, for such reactions are believed to occur at the interface.^{1–4}

Room-temperature ionic liquids, which are composed of ions and are fluid over a wide range of temperatures (<100 °C), are finding increasing applications due to their unique physical and chemical properties.^{5,6} These properties include high thermal stability, high ionic conductivity, negligible vapor pressure, and increased electrochemical window.^{6–9} Due to these properties, this class of compounds has been used in quite a number of applications which include reaction media for synthesis, liquid–liquid extraction, and biphasic catalysis.^{1,3–5,10–15} Furthermore, their wide electrochemical windows allow them to be used as solvents in electrochemistry and spectroscopic studies.^{4,6,16} In addition, their properties can easily be tuned by changing one of the ions.^{17–21} Another promising application for the liquid salts is in the gas separation process.^{22–25} Studies have shown that ionic liquids show good potential as gas separation media and having negligible volatility is an advantage over the traditional organic solvents in absorption of gases.^{22–25} The first step in the gas capture process takes place at the interface, with the first layer of molecules in the liquid phase interacting with the gas molecules; it is therefore significant to the understanding of the mechanisms of gas absorption. Hence, study of the interfacial structure of ionic liquids at the gas–liquid interface is relevant. Furthermore, for advances in this field, characterization of the ionic liquid surface at the molecular level is important as the surface composition and structure govern the physical and chemical properties of the material.

Recent studies on the surface orientation and composition of ionic liquids have been possible using a range of experimental techniques such as surface tension measurements,^{20,26–30} X-ray photoelectron spectroscopy,^{31–33} ion scattering and recoil spectroscopy,^{34–36} X-ray reflectivity,³⁷ neutron reflectometry,³⁸ and nonlinear spectroscopy such as sum-frequency generation,^{39–43} as well as computer simulations.^{44–48} Studies based on X-ray crystallography have also been carried out to determine the structure and interactions among these ions to further understand their behavior.^{49–56} However, results from these surface techniques do not agree with one another. Questions, such as how the ions are oriented at the surface and which ions occupy the

top layer of the gas–liquid interface, remain open. In this paper we address these questions by using surface-specific vibrational spectroscopy, sum-frequency generation (SFG). Using SFG, the surface orientation of the anion and cation of the ionic liquid at the gas–liquid interface is determined. The results are supported by X-ray diffraction of the solidified bulk ionic liquid, which determines the relative orientation of ions in the bulk liquid. In addition, the crystal-like behavior of the ionic liquid surface offers substantial information regarding the surface location of both the cation and anion relative to one another in the liquid phase.

In this study, the orientation and interfacial location of the ions 1-butyl-3-methylimidazolium, [BMIM]⁺, cation and methyl sulfate, [MS][−], and methanesulfonate, [CH₃SO₃][−], anions at the gas–ionic liquid interface have been determined by SFG spectroscopy and X-ray crystallography.

Background

SFG has been successfully applied as a surface probe for the characterization of interfaces at a molecular level due to its high surface sensitivity. The high surface sensitivity arises because SFG is only allowed in media with noncentrosymmetric environments such as surfaces or interfaces where the centrosymmetric structure is broken. Molecules in the bulk liquid state are considered to be in an isotropic environment; hence, SFG is forbidden. SFG theory has been described thoroughly in several papers.^{57–60}

Generally, SFG experiments involve overlapping two laser beams (one with tunable IR frequency and the other with visible light frequency) on the surface of the material, generating a third beam with a frequency equal to the sum of the two incident beams. The intensity of the SFG signal, $I(\omega_{\text{SF}})$, is proportional to the square of the induced polarization, where E refers to the electric fields of the incoming visible and IR beams as indicated in eq 1. $\chi^{(2)}$ is the second-order nonlinear susceptibility that relates the interface response to the two input light fields. According to eq 2,

$$I(\omega_{\text{SF}}) \propto |P^{(2)} = \chi^{(2)}:E_{\text{vis}}E_{\text{IR}}|^2 \quad (1)$$

$$\chi^{(2)} = \frac{N\langle\beta^{(2)}\rangle}{\omega_{\text{IR}} - \omega_n + i\Gamma_n} \quad (2)$$

the nonlinear susceptibility contains all the information on the molecule through the hyperpolarizability, $\beta^{(2)}$, containing contributions from the Raman polarizability and IR dipole transition and averaged over the molecule orientation as indicated by angular brackets. N indicates the number of modes contributing to the SFG signal, ω_{IR} and ω_n refer to the frequencies of the incoming IR and the normal mode, respectively, and Γ_n is the damping constant.

By using different polarization combinations of incoming and outgoing laser beams, the molecular orientation tilt angle (θ) of the surface molecules with respect to the surface normal can be deduced by using the polarization intensity ratio (PIR) method, which is the conventional way of determining the orientation of the molecular group at the surface.^{42,61–65}

Recently, Wang et al.^{66–69} have reformulated the analysis of SFG data for orientation analysis in terms of the SFG polarization null angle (PNA) as opposed to the usual PIR method. They have shown that there exists a situation where, by analyzing the output polarization angle (Ω_{sf}) with inputs of -45° (Ω_{vis}) for the visible and 0° (Ω_{IR}) for the infrared, the SFG signal goes to zero at a given orientation tilt angle and Ω_{sf} . The null angle is measured at a certain frequency (peak position) by mapping the intensities at different polarization angles of the sum-frequency signal; the minimum in the curve is taken as the null angle in which the sum-frequency signal is taken to be zero.^{66–69}

The polarization intensity ratio is the traditionally used method to determine the molecular orientation of functional groups at the interface.^{61,63} It involves the measurement of the ratios of the experimental peak amplitudes at a certain vibrational mode with different polarization combinations. The peak amplitudes are derived from curve fitting of the SFG data. However, as this is based on the peak amplitudes, the tilt angle values may be inaccurate, as some vibrations have a weak signal in one polarization combination.⁶⁸ On the contrary, the polarization null angle is an alternative method of quantitatively analyzing the orientation of the functional group at the surface and can be applied to systems where the PIR method is not feasible.⁶⁷ It sometimes offers a more reliable orientation analysis.⁶⁸

The sensitivity of the PNA method depends significantly on the SFG experimental configuration, which was found to be highly suitable and efficient for the copropagating configuration. Furthermore, Wang et al.⁶⁸ have verified that the optimal condition for the polarization analysis is where the incident angles of both the IR and visible beams are around $50\text{--}70^\circ$, which gives the strongest SFG intensity. On the basis of the given conditions, our system is well suited for the PNA measurements.

PNA improves the accuracy of the tilt angle value compared to the PIR method. Previous SFG experiments have determined the tilt angles to be 54° and 47° for the CH_3 group of the butyl chain in [BMIM][PF₆] and [BMIM][Br], respectively, using the PIR method.⁴² An analogous experiment has been carried out by Kim et al.³⁹ They reported a tilt angle of $<38^\circ$ for [BMIM][PF₆].³⁹ A null angle measurement for [BMIM][PF₆] was performed and gave a tilt angle of 59° .⁷⁰ However, the PNA method also has its own limitations. It will fail if the considered peak has some contributions from other vibrational modes or spectral interference and peak overlap. In this instance, a careful spectral fitting is necessary to obtain an accurate Ω_{null} .^{68,69} In this paper, only the single isolated peaks were analyzed.

Experimental Section

Sample Preparation. The synthesis of 1-butyl-3-methylimidazolium methyl sulfate followed the procedure published previously.⁴⁹ It consists of alkylating 1-butylimidazole with dimethyl sulfate in toluene while keeping the temperature below 40°C as the reaction is very exothermic. 1-Butyl-3-methylimidazolium methanesulfonate was synthesized according to the procedure described previously.⁷¹ This involves the reaction between 1-butyl-3-methylimidazolium chloride and methanesulfonic acid with 1-propanol. The reaction was run at 100°C , with chloropropane being removed through a distillation process. Both ionic liquids were characterized using ¹H NMR spectroscopy. The chemicals were from Sigma-Aldrich and used without further purification except 1-butylimidazole, which was distilled prior to use.

The ionic liquid was dried under high vacuum prior to each experiment. It was transferred to the glass SFG cell with Kalrez O-rings and Teflon stopcocks. The sample was dried at $\sim 70^\circ\text{C}$ in a glass vacuum line equipped with liquid nitrogen traps until the pressure reached 5×10^{-5} Torr. The cell was then backfilled with argon gas prior to the SFG experiment.

SFG Spectroscopy. The spectra for [BMIM][MS] were acquired at room temperature, while [BMIM][CH₃SO₃] was heated at $\sim 70^\circ\text{C}$ as this is solid at room temperature. Each spectrum was averaged over 5 scans with 20 shots/point at $1\text{ cm}^{-1}/\text{s}$. The experimental data were corrected for IR fluctuations, and the peak intensity was normalized relative to the CH₃ symmetric stretch peak in the ssp (s-polarized SFG, s-polarized vis, and p-polarized IR) spectrum of the sample. The fitting of the final SFG spectra was performed with Origin 7.0 Professional nonlinear curve fitting using eqs 1 and 2 in the fitting function with the instrumental setting method for the error bars.

X-ray Structure Determinations. Single crystals of [BMIM][CH₃SO₃] were obtained upon slow cooling of the melt to room temperature in the oil bath under nitrogen. Crystals of [BMIM][MS] were obtained from liquid [BMIM][MS] in a freezer at -20°C . All manipulations with crystals have been performed at a temperature below -20°C in a nitrogen atmosphere. Single-crystal X-ray diffraction data were collected with the use of graphite-monochromatized Mo K α radiation ($\lambda = 0.71073\text{ \AA}$) at 173 K on a Bruker Smart 4K CCD diffractometer.⁷² Data were collected by a scan of 0.3° in ω in four sets of 606 frames at φ settings of 0° , 90° , 180° , and 270° . The exposure times were 10 s/frame. The collection of the intensity data was carried out with the program SMART.⁷² Cell refinement and data reduction were carried out with the use of the program SAINT.⁷² Then the program SADABS⁷² was employed to make incident beam and decay corrections. The structures were solved with the direct methods program SHELXS and refined with the full-matrix least-squares program SHELXTL of the SHELXTL suite of programs.⁷³ The positions of the hydrogen atoms were idealized and constrained with the use of a riding model. The final models involved anisotropic displacement parameters for all non-hydrogen atoms.

Results

SFG Polarization Spectra. Polarization data for [BMIM][MS] and [BMIM][CH₃SO₃] are shown in Figures 1A and 2A, respectively. The vibrational mode assignments and their corresponding frequencies are summarized in Table 1. Peak assignments for the vibrational modes of the butyl chain are based on the IR study of long alkyl chain compounds,^{74,75} while modes for the methyl sulfate and methanesulfonate anions are assigned on the basis of the SFG studies of methanol,^{76,77} IR

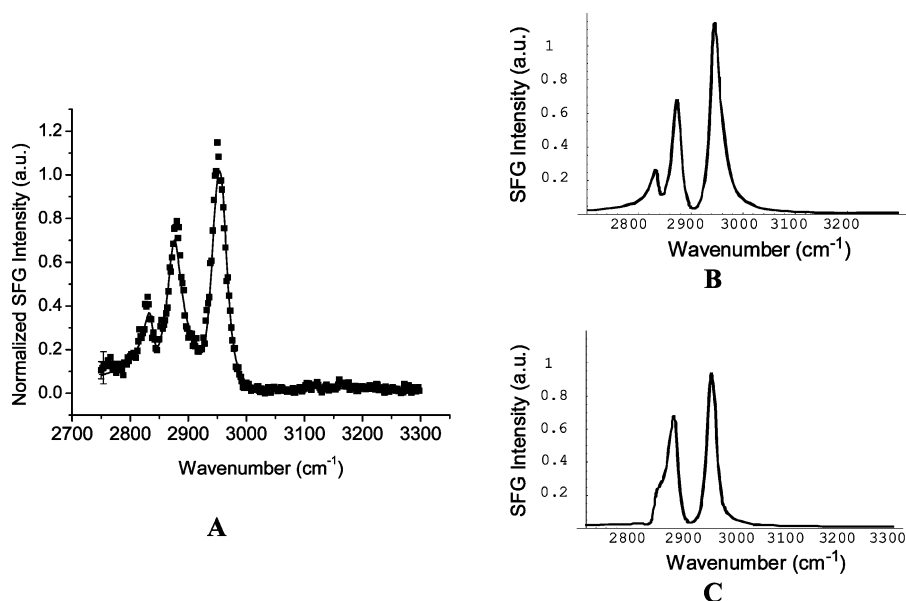


Figure 1. SFG spectra of [BMIM][MS] ssp polarization: (A) experimental SFG spectrum of [BMIM][MS] ssp polarization; (B) simulation with $\chi(2)_{\text{MS}}$ of the same sign as that of $\chi(2)_{\text{CH}_3}$; (C) simulation with $\chi(2)_{\text{MS}}$ of sign opposite to that of $\chi(2)_{\text{CH}_3}$.

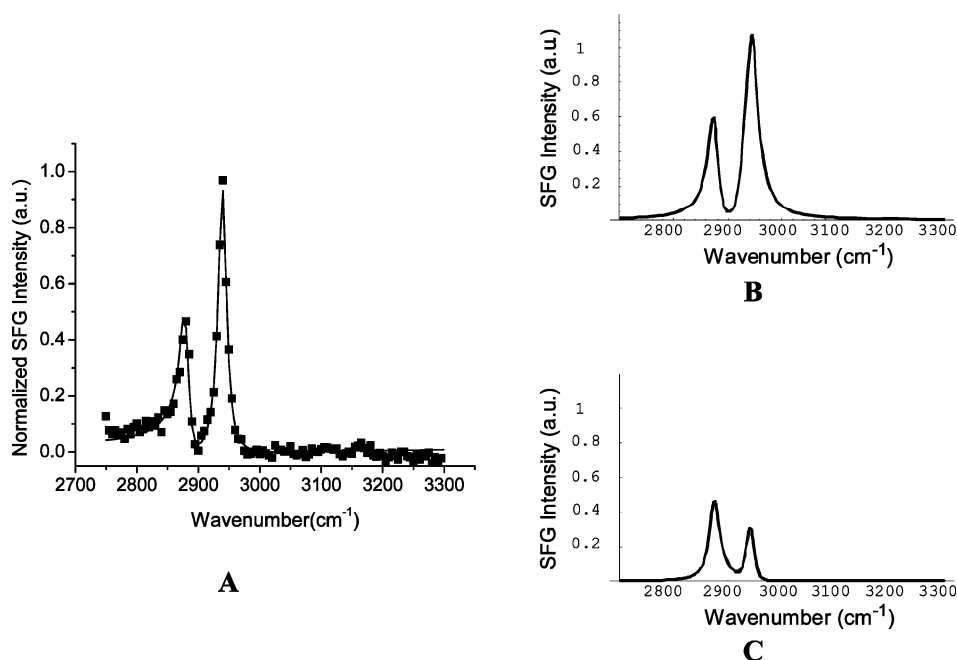


Figure 2. SFG spectra of [BMIM][CH₃SO₃] ssp polarization: (A) experimental SFG spectrum of [BMIM][CH₃SO₃] ssp polarization; (B) simulation with $\chi(2)_{\text{CH}_3-\text{CH}_3\text{SO}_3}$ of the same sign as that of $\chi(2)_{\text{CH}_3}$; (C) simulation with $\chi(2)_{\text{CH}_3-\text{CH}_3\text{SO}_3}$ of sign different from that of $\chi(2)_{\text{CH}_3}$.

TABLE 1: C–H Stretching Mode Assignments for [BMIM][MS] and [BMIM][CH₃SO₃]

peak assignment	frequency (cm ⁻¹)		
	[BMIM] ⁺	[MS] ⁻	[CH ₃ SO ₃] ⁻
$\nu_{\text{s}}(\text{CH}_3)^{74,75}$	~2878		
$\nu_{\text{CH}_3-\text{FR}}^{74,75}$	~2945		
$\nu_{\text{s}}(\text{CH}_3-\text{MS})^{76,77}$		~2825	
$\nu_{\text{MS}-\text{FR}}^{76,77}$		~2915	
$\nu_{\text{s}}(\text{CH}_3-\text{CH}_3\text{SO}_3)^{78-81}$ $\nu_{\text{CH}_3-\text{FR}}^{74,75}$			~2939

and Raman studies of ethyl methanesulfonate⁷⁸ and methanesulfonate salts,^{79,80} and the SFG study of methanesulfonic acid.⁸¹ All the peaks in the spectra are associated with the terminal methyl group of the butyl chain of the [BMIM]⁺ cation and the methyl groups from the methyl sulfate and methanesulfonate anions.

[BMIM][MS]. Three distinct peaks are observed in the ssp spectrum (Figure 1A) of [BMIM][MS]. Four vibrational modes contribute to these peaks, which are due to the C–H symmetric stretches of the methyl group from the methyl sulfate anion, $\nu_{\text{s}}(\text{CH}_3-\text{MS})$, and the methyl group at the end of the butyl chain, $\nu_{\text{s}}(\text{CH}_3)$, and their corresponding Fermi resonances, $\nu_{\text{MS}-\text{FR}}$ and $\nu_{\text{CH}_3-\text{FR}}$. The vibrations at ~2825 and ~2878 cm⁻¹ are assigned to $\nu_{\text{s}}(\text{CH}_3-\text{MS})^{76,77}$ and $\nu_{\text{s}}(\text{CH}_3)^{74,75}$ respectively. The peak at ~2945 cm⁻¹ is believed to have contributions from the Fermi resonances of both CH₃ symmetric stretches. This conclusion is reached on the basis of the previous results in our laboratory^{41–43} for ionic liquids based on [BMIM]⁺ with an anion without a C–H stretch mode (e.g., [PF₆]⁻ and [BF₄]⁻). The peaks in the ssp spectra for these compounds do not have the same intensity as the ~2945 cm⁻¹ peak observed here.^{41–43}

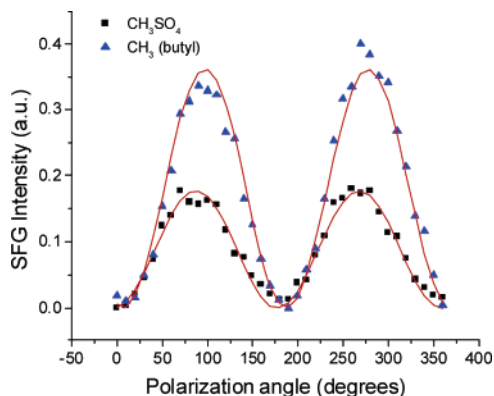


Figure 3. Polarization null angle for CH₃ of methyl sulfate (black squares) and (blue triangles) CH₃ of the butyl chain.

[BMIM][CH₃SO₃]. Two strong discernible peaks are observed in the ssp spectrum (Figure 2A). The $\sim 2878\text{ cm}^{-1}$ mode is $\nu_{\text{s(CH}_3\text{)}}$ as assigned above, while the peak at $\sim 2939\text{ cm}^{-1}$ actually has contributions from two modes, the CH₃ symmetric stretch of the methanesulfonate anion, $\nu_{\text{s(CH}_3\text{-CH}_3\text{SO}_3)}$ ^{78–81} and $\nu_{\text{CH}_3\text{-FR}}$.^{74,75} The CH₃ antisymmetric stretch from the methanesulfonate, which is at $\sim 3024\text{ cm}^{-1}$, and the Fermi resonance have not been observed in any polarization data.^{79,80} The CH₃ antisymmetric deformation mode typically occurs at 1426 cm^{-1} ; thus, its overtone would be expected at 2852 cm^{-1} .^{79,80} As the difference between the CH₃ symmetric mode, 2939 cm^{-1} , and the overtone, 2852 cm^{-1} , is relatively large, this may likely be an explanation for the absence of the Fermi resonance in any polarization data. In fact, from the Raman and IR studies of Seshadri et al.⁸⁰ and Thompson⁷⁹ on methanesulfonate salts, e.g., NaCH₃SO₃, LiCH₃SO₃, and CsCH₃SO₃, the Fermi resonance has not been observed.

Imidazolium ring modes, which appear at ~ 3150 and $\sim 3175\text{ cm}^{-1}$ for antisymmetric and symmetric H–C(4)–C(5)–H stretches, respectively, and at $\sim 3130\text{ cm}^{-1}$ for the H–C(2) symmetric stretch, are not observed for both ionic liquids.⁸²

Orientation by the Polarization Null Angle. Orientation analysis by the polarization null angle is accomplished by reformulating eqs 1 and 2, so that the SFG intensity is a function of the tilt angle, θ , and the output polarization. For each given tilt angle, the null angle occurs at a different polarizer setting. From this graph, a comparison between the measured null angle and the calculated curve is made to determine the molecular tilt angle from the surface normal. The y axis range in the theoretical plots in Figure 3 is limited to show the detail at the curve minimum, and the full curves display the sinusoidal shape as in the polarization null angle data.

The null angle measurements for the symmetric stretch vibration of the methyl group from the methyl sulfate and the butyl chain are shown in Figure 3. The minimum for $\nu_{\text{s(CH}_3\text{-MS)}}$ is at $2^\circ \pm 3^\circ$, and that for $\nu_{\text{s(CH}_3\text{)}}$ is at $10^\circ \pm 2^\circ$. Figure 4 shows the theoretical plots of the polarization null angle for [BMIM][MS]. The average tilt angle is given by the minimum in the polarization curve. The peak overlap between the vibrational modes of $\nu_{\text{CH}_3\text{-FR}}$ and $\nu_{\text{s(CH}_3\text{-CH}_3\text{SO}_3)}$ prohibits the PNA measurement of $\nu_{\text{s(CH}_3\text{-CH}_3\text{SO}_3)}$.

X-ray Structure. [BMIM][MS] crystallizes in monoclinic space group $P2_1/c$ with $a = 8.6241\text{ \AA}$, $b = 20.8231\text{ \AA}$, $c = 7.9666\text{ \AA}$, and $\beta = 113.384^\circ$. The molecular structure of [BMIM][MS] is shown in Figure 5. The imidazolium ring is planar, with the C(6) and C(7) atoms deviating by 0.030 and 0.018 Å from the plane of the ring, respectively. The remainder of the butyl chain propagates in an *all-trans* conformation with

a N1–C7–C8–C9 torsion angle of 62.4° . The four carbons of the butyl group lie in a plane (within experimental error) which is positioned at an 85.2° angle to the imidazolium ring. The C(9)–C(10) line (C3 axis) of the methyl has a tilt of approximately 37.8° with respect to the imidazolium ring (from SFG data, the imidazolium ring is taken to be parallel to the surface plane), with the C(10) carbon atom positioned 3.751 \AA above the imidazolium ring. The distance between the center of the imidazolium ring and the center of the SO₄[−] moiety is 3.996 \AA . The methyl sulfate anion is tilted with respect to the imidazolium ring, with the O(4)–C(11) line being 48.9° to the normal of the imidazolium ring. The crystal packing of [BMIM][MS] along the crystallographic axis a is presented in Figure 6.

[BMIM][CH₃SO₃], on the other hand, crystallizes in triclinic space group $P\bar{1}$ with $a = 7.9343\text{ \AA}$, $b = 8.4797\text{ \AA}$, $c = 10.2782\text{ \AA}$, $\alpha = 103.404^\circ$, $\beta = 99.567^\circ$, and $\gamma = 111.620^\circ$. The molecular structure of [BMIM][CH₃SO₃] is shown in Figure 7. Like in [BMIM][MS], the imidazolium ring in [BMIM][CH₃SO₃] is also planar, with the C(6) and C(7) atoms deviating by 0.050 and 0.064 Å from the plane of the ring, respectively. The butyl chain propagates in an *all-trans* conformation with a N1–C7–C8–C9 torsion angle of 63.8° . The four carbons of the butyl group lie in a plane (within experimental error), which is positioned at an 84.6° angle to the imidazolium ring. The C(9)–C(10) bond is positioned at 42.0° to the normal of the imidazolium ring, with the C(10) carbon atom positioned 3.576 \AA above the imidazolium ring. The distance between the center of the imidazolium ring and the center of the SO₃[−] moiety of the closest anion is 3.823 \AA . The methanesulfonate anion is tilted with respect to the imidazolium ring, with the S(1)–C(11) bond being at 47.6° to the normal of the imidazolium ring. The crystal packing of [BMIM][MS] along the crystallographic axis a is presented in Figure 8.

Discussion

Orientation calculations were performed for the methyl groups at the end of the butyl chain and from the methyl sulfate anion, which is assumed to have C_{3v} symmetry. Figure 4 shows the theoretical plots of PNA measurements with their corresponding tilt angles for [BMIM][MS]. The tilt angle of the methyl group from the methyl sulfate is analyzed to be 62° , which is nearly parallel to the surface plane. The orientation of the methyl group at the end of the butyl chain is determined to be near 53° from the surface normal. The null angle of $\nu_{\text{s(CH}_3\text{)}}$ is similar for [BMIM]⁺ in all ionic liquids; thus, it has the same orientation.^{42,70} Furthermore, $A_{\text{CH}_3(\text{sym})}/A_{\text{CH}_3(\text{FR})} = 1.5$ for [BMIM]⁺. This ratio is important for orientation determination based on phase analysis. However, the null angle of the CH₃ group of the methanesulfonate was not measured, as this peak is overlapped with the resonance of $\nu_{\text{CH}_3\text{-FR}}$ of the butyl chain.

With the methyl group from the butyl chain, $\nu_{\text{s(CH}_3\text{)}}$, established to be oriented away from the bulk liquid, the relative sign of the susceptibility can be determined to verify the phase of other normal modes.⁸³

SFG spectra are described by the second-order susceptibility, $\chi^{(2)}$, by the following relation for [BMIM][MS]:

$$I_{\text{SF}} \propto |\chi_{\text{CH}_3}^{(2)} + \chi_{\text{CH}_3\text{-FR}}^{(2)} + \chi_{\text{MS-CH}_3}^{(2)} + \chi_{\text{MS-FR}}^{(2)}|^2$$

The subscripts indicate the vibrational modes contributing to the signal, which are due to the symmetric stretch vibration and Fermi resonance of the methyl group at the end of the butyl chain^{74,75} and the CH₃ symmetric stretch and Fermi resonance of the methyl sulfate anion.^{76,77} The shape of the SFG spectrum

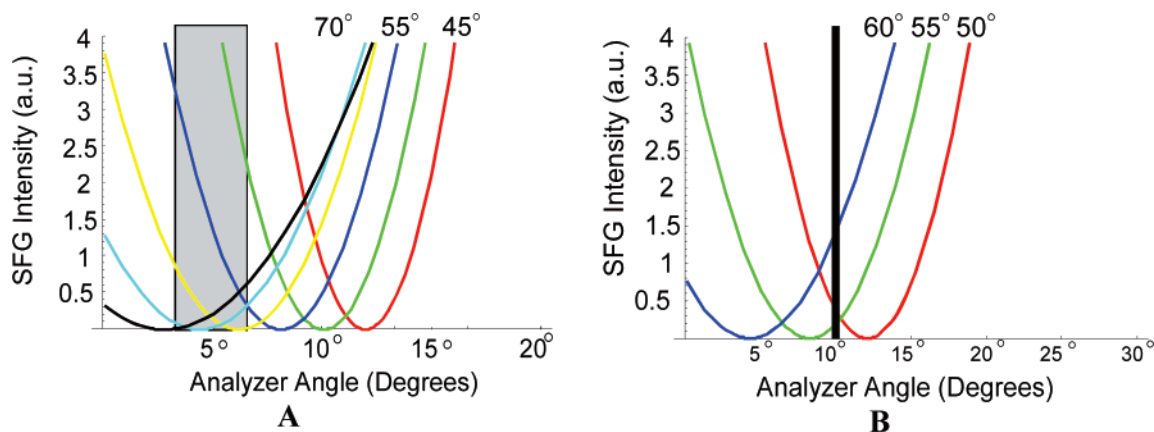


Figure 4. Theoretical plots of the polarization null angle for [BMIM][MS]: (A) CH₃ of methyl sulfate, red → black, $\theta = 45^\circ \rightarrow 70^\circ$, $\Delta 5^\circ$; (B) CH₃ of butyl, red → blue, $\theta = 50^\circ \rightarrow 60^\circ$, $\Delta 5^\circ$. The solid vertical bar indicates the measured null angle value.

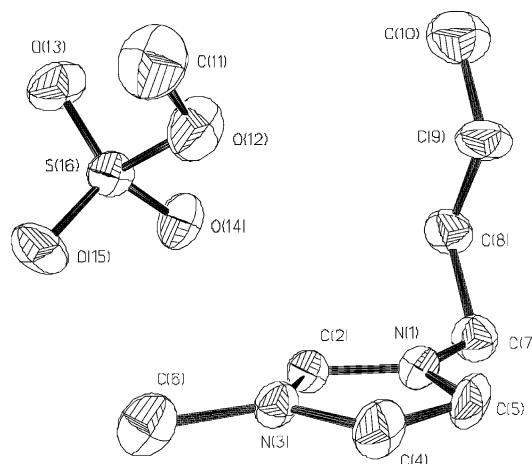


Figure 5. Molecular structure of [BMIM][MS]. Hydrogens are omitted for clarity.

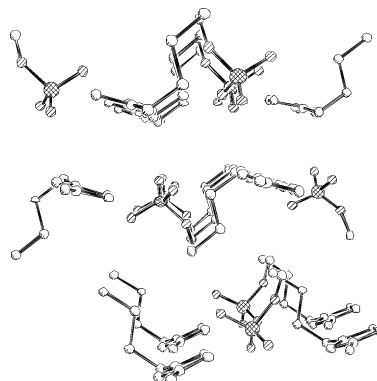


Figure 6. Packing of [BMIM][MS] along the *a* axis.

is sensitive to the phase or the sign of each susceptibility contributing to it.⁵⁷ Further, the sign of the susceptibility is related to the orientation of the functional group.^{83,84} The relationship is relative to a known phase reference; once the phase of one mode is set, then other modes can be compared to it and the up or down directionality with respect to the surface plane inferred.^{83,84} In the ionic liquid system presented here, the CH₃ group of the butyl chain is considered to be directed away from the bulk liquid into the vapor phase. $\chi_{\text{CH}_3}^{(2)}$ (from butyl) is given a positive sign. The SFG spectrum of [BMIM][MS] is presented in Figure 1A. Figure 1B shows the simulated spectrum in which $\chi_{\text{MS-CH}_3}^{(2)}$ (and $\chi_{\text{MS-FR}}^{(2)}$) is given a positive sign, the same as for $\chi_{\text{CH}_3}^{(2)}$ (and $\chi_{\text{CH}_3\text{-FR}}^{(2)}$). This simulation agrees well with the experimental results in terms of peak

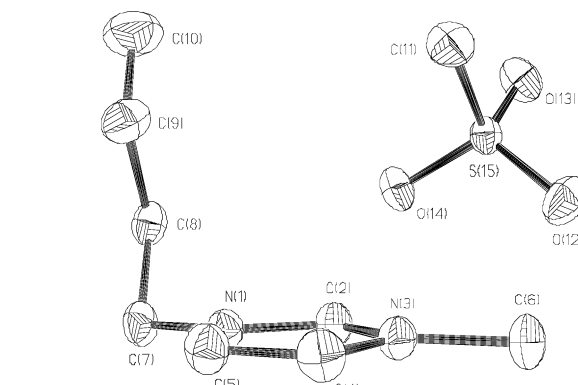


Figure 7. Molecular structure of [BMIM][CH₃SO₃]. Hydrogens are omitted for clarity.

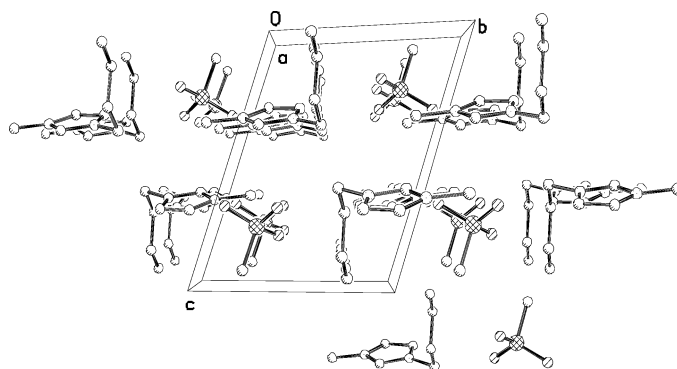


Figure 8. Packing of [BMIM][CH₃SO₃] along the *a* axis.

positions, spectral shape, and relative intensity between the peaks. The spectrum in Figure 1C, on the other hand, uses the same parameters as the simulation in Figure 1B; however, $\chi_{\text{MS-CH}_3}^{(2)}$ (and $\chi_{\text{MS-FR}}^{(2)}$) has a sign opposite that of $\chi_{\text{CH}_3}^{(2)}$ (and $\chi_{\text{CH}_3\text{-FR}}^{(2)}$). This simulation leads to a spectrum that is very different from the experimental spectrum. For instance, this spectrum shows four peaks, but since they are very close in intensity and wavelength, they would not be resolved with the SFG spectrometer ($\Delta\nu \approx 5 \text{ cm}^{-1}$) and would appear as two peaks instead. This clearly shows that the simulation for which the susceptibilities from methyl sulfate and the butyl chain having the same sign is more comparable to the experimental spectrum than the simulation where they have opposite signs. This is evidence for the direction of the methyl groups at the surface.

A similar procedure is applied to [BMIM][CH₃SO₃] with the following relation:

$$I_{\text{SF}} \propto |\chi_{\text{CH}_3}^{(2)} + \chi_{\text{CH}_3\text{-FR}}^{(2)} + \chi_{\text{CH}_3\text{-CH}_2\text{SO}_3}^{(2)}|^2$$

The contribution to the signal is from the vibrational modes due to the CH₃ symmetric stretch of the methanesulfonate anion and from the butyl chain. The CH₃ symmetric stretch of the methanesulfonate is overlapped with $\nu_{\text{CH}_3\text{-FR}}$ of the butyl; however, since the contribution to this peak from $\nu_{\text{CH}_3\text{-FR}}$ is known, which is determined from the ratio as mentioned above ($A_{\text{CH}_3(\text{sym})}/A_{\text{CH}_3(\text{FR})} = 1.5$), the remaining amplitude is extracted by peak fitting analysis. Since the contribution of the methyl group from the butyl chain is known and is confirmed to be directed away from the bulk liquid, the remaining intensity of the $\sim 2939 \text{ cm}^{-1}$ peak is therefore due to the methanesulfonate, and this may add either constructively or destructively. If the methanesulfonate adds destructively, this implies that the CH₃ group is directed into the bulk liquid, while if it adds constructively, the CH₃ group is pointed into the vapor phase as in the case of the CH₃ group from [BMIM]⁺. A simulation of both situations is presented in Figure 2B,C. Using the known amplitude ratio of the methyl group on the butyl chain, the remaining amplitude at 2939 cm^{-1} is attributed to the CH₃ symmetric stretch (of methanesulfonate).⁷⁸ Figure 2B illustrates the simulated spectrum of $\chi_{\text{CH}_3\text{-CH}_2\text{SO}_3}^{(2)}$ with the same sign as $\chi_{\text{CH}_3}^{(2)}$ ($\chi_{\text{CH}_3\text{-FR}}^{(2)}$), which is positive. The simulation results suggested that the CH₃ group of the methanesulfonate is also pointing away from the surface, as in the case of the CH₃ group at the end of the butyl chain. This phase simulation enables the determination of the polar orientation of the methyl group at the surface.

Crystallographic data, on the other hand, might be used as a guide in considering the surface composition of the ionic liquids. X-ray crystallography provides insight into the crystal structure and physical properties of ionic liquids at a molecular level.⁸⁵ Modification of the properties of these salts within the solid and liquid states requires a model, which possesses valid interionic interactions to be able to develop various plausible approaches. Therefore, the crystal structures of ionic liquids are important because they provide the basis in understanding the structural organization of ions in the liquid state.⁸⁶ Previous studies comparing the crystal and liquid structures of short-chain 1,3-dimethylimidazolium chloride and hexafluorophosphate salts revealed a strong correlation between the solid and liquid structures.^{87,88} Even for the longer alkyl chain salts, e.g., [C₁₂MIM][Cl], Bradley et al.⁸⁹ suggested that the structures of the crystal and liquid crystalline regions might be used to describe that of the liquid. Other studies include [EMIM][PF₆],⁵¹ the halide salts of *n*-butyl chain analogues, [BMIM][Cl] and [BMIM][Br],⁵² and other longer chain salts, [C₁₂MIM][PF₆] and [C₁₄MIM][BF₄],^{50,56} all have melting points above room temperature. The short-chain salts have high melting points due to the dominance of the strong cation–anion interactions. The halide salts, e.g., [BMIM][Cl] and [BMIM][Br], have substantial hydrogen bonding, while the long-chain analogues have significant alkyl chain hydrophobic interactions that also lead to high melting points. Therefore, the comparison of the crystalline and liquid structures of these salts may be compromised for the above-mentioned interactions. However, a recent study on 1-butyl-3-methylimidazolium hexafluorophosphate ionic liquid suggested that the structure obtained from a single crystal is very much like the local structure of this ionic liquid in its fluid state.⁵⁴ This salt is liquid at room temperature with a weakly coordinating [PF₆][−] anion. Further, the electron densities of the surface layer of the liquid and the bulk crystalline sample were compared and suggested that the study of the solid-state structure

can greatly facilitate the elucidation of the structural features of ionic liquids not only in the bulk liquid but also at the liquid surface.^{37,54} Although crystal structures of 1-alkyl-3-methylimidazolium ionic liquids^{50–53,55,56,89,90} have been published, there is no structure reported for the corresponding methanesulfonate salt. A crystal structure of pyridinium methanesulfonate however has been reported, which shows weak hydrogen bonding between the ring hydrogen protons and the three oxygen atoms of the methanesulfonate anion, but the only reported significant hydrogen bonding is between NH and one of the three oxygen atoms.⁹¹ For the methyl sulfate salt, the only crystal structure reported is for the 1,3-dimethylimidazolium, [MMIM], ionic liquid.⁴⁹ The structure shows significant hydrogen-bonding interactions between the imidazolium ring protons and the three terminal oxygen atoms of the anion, which form the intraribbon hydrogen bonds. However, no significant interribbon hydrogen bonds are observed, which may account for its lower melting point ($43 \text{ }^\circ\text{C}$) compared to its chloride salt counterpart ($65 \text{ }^\circ\text{C}$).⁵ For the two compounds considered here, all the interactions that involve the ring protons and the oxygen atoms are smaller than the sum of the van der Waals radii of hydrogen (1.2 \AA) and oxygen (1.52 \AA) by 0.2 \AA . These are considered very weak hydrogen bonds in crystal structures.⁵¹ Figure 9 and Table 2 show the hydrogen-bonded chains and the distances and angles in the crystal structures of both salts, respectively. In contrast to 1,3-dimethylimidazolium methyl sulfate, [MMIM][MS], [BMIM][MS] does not exhibit any substantial hydrogen bonding, which may be attributed to the chain length difference in the cation of these two compounds. The butyl chain disrupts the strong interaction between the cation and anion, hence the lower melting point which is reported to be $-5 \text{ }^\circ\text{C}$.⁴⁹ In general, the proton in the C(2) position is prominent in forming the hydrogen bond since it is the most acidic, as observed in [BMIM][PF₆] (the H–F distance is 2.36 \AA).⁵⁴ In this work, [BMIM][MS] does not even exhibit that interaction, which is surprising, and in [BMIM][CH₃SO₃], the distance is 2.48 \AA . In fact, only protons from the CH₃ group attached to the nitrogen atom are involved in the interaction in [BMIM][MS]. Hydrogen bonds that involve alkyl protons are considered very weak interactions. Therefore, [BMIM][CH₃SO₃] is better in forming hydrogen bonds than [BMIM][MS]. In fact, [BMIM][CH₃SO₃] packs in sheets, thereby forming a two-dimensional array, as opposed to one-dimensional chain packing in [BMIM][MS]. In addition, the methanesulfonate anion is more compact and more suitable for packing than the large and bent methyl sulfate anion. [BMIM][CH₃SO₃] is, in fact, solid at room temperature, with an estimated melting point between 60 and $65 \text{ }^\circ\text{C}$.

While X-ray diffraction studies provide structural information on the bulk crystalline material, SFG spectroscopy provides orientation information on the functional groups present at the surface. Although the structural organization of the bulk liquid is random in comparison with that of the solid state, studies have shown good correlation between the crystalline and liquid structures of the low melting point salts, as mentioned earlier.^{87–89,92} However, the molecular environment at interfaces is different from that of the bulk material due to the differences in the forces experienced by the molecules in the bulk and at the surface.⁹³ The molecules at the surface layer are subjected to unbalanced forces as they are in contact with fewer molecules. Since surface molecules in liquid are free to move, they can orient and arrange themselves in such a way as to keep the surface energy of the system at its minimum.^{93–96} According to Langmuir's principle, the measured surface energy or surface tension corresponds to the part of the molecule that is present

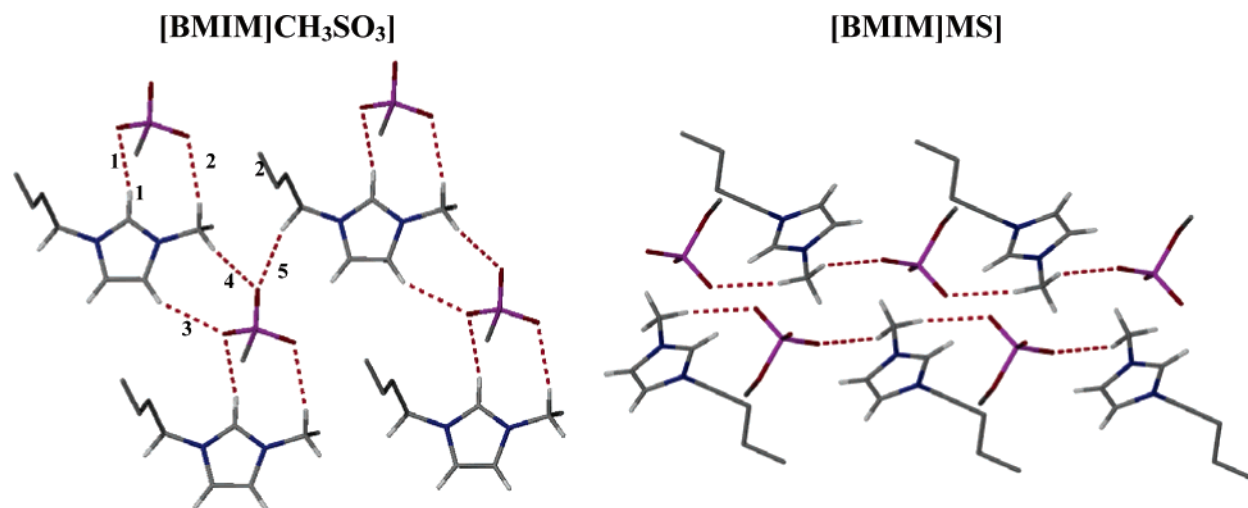


Figure 9. Crystal structures of [BMIM][CH₃SO₃] and [BMIM][MS] showing hydrogen-bonded chains.

TABLE 2: Hydrogen-Bonding Distances and Angles from [BMIM][CH₃SO₃] and [BMIM][MS] Crystal Structures

	H–O (Å)	O–C (Å)	C–H–O angle (deg)
[BMIM][CH ₃ SO ₃]			
1	2.478	3.279	142.03
2	2.385	3.308	156.70
3	2.476	3.300	145.04
4	2.334	3.300	168.66
5	2.498	3.384	148.73
[BMIM][MS]			
1	2.362	3.320	165.55
2	2.517	3.429	154.7

at the interface.^{93–96} From the SFG results, only methyl groups at the end of the butyl chain and from the anion are observed in the spectra, which suggests that hydrocarbon chains are closer to the gas–ionic liquid interface than their head groups.

The surface composition of the ionic liquids is also suggested by surface tension measurements. Unfortunately, surface tension data are still limited, and no data have been reported yet for the salts considered in this study. However, the surface tension of a shorter chain analogue, 1-ethyl-3-methylimidazolium ethyl sulfate ([EMIM][EtSO₄]), was reported by Wilkes et al.²⁸ and Xu et al.⁹⁷ Wilkes et al.²⁸ measured the surface tension at room temperature using the capillary rise method for several ionic liquids based on the 1-alkyl-3-methylimidazolium cation. They have also tabulated representative published surface tensions of imidazolium-based ionic liquids and found a significant discrepancy among the reported values. In addition, four of the compounds that they studied also showed a discrepancy from previous results. For instance, their measured surface tension of [EMIM][EtSO₄] is 42.5 dyn/cm⁻¹ as opposed to 48.79 dyn/cm⁻¹ reported by Xu et al.⁹⁷ Wilkes et al.²⁸ measured the surface tension of the compound under ambient conditions and yielded a 52.4 dyn/cm⁻¹ value, which is closer to the measurement obtained by Xu et al.⁹⁷ They attributed the difference to drying precautions. Inconsistency in the reported values might be due to a number of sources, e.g., the presence of moisture in the ionic liquid or some contaminants.

While the presence of an alkyl chain coincides with the reduction of the surface tension of a given compound, it is therefore interesting to compare the surface tensions of [EMIM]-[EtSO₄] and [EMIM][BF₄].^{93,95} From the measurements of Wilkes et al.,²⁸ [EMIM][BF₄] has a surface tension of 44.3 dyn/cm, which is noticed to be slightly higher than the 42.5 dyn/cm of [EMIM][EtSO₄]. It is logical to compare the surface tension

of a relatively longer butyl chain on the cation, e.g., [BMIM]-[BF₄], with that of [EMIM][BF₄] for further comparison, but Wilkes et al.²⁸ have not measured the surface tension of [BMIM]-[BF₄]. Although other groups have previously reported the surface tension of [BMIM][BF₄], the results are not in agreement with one another as noted by Wilkes et al.²⁸ in their recent study. A decrease in the surface tension was observed upon increasing the chain length ($n = 4, 6, 8$) on the imidazolium cation for a common anion as shown from the measurements of Watson et al.²⁰ On the other hand, keeping the alkyl chain length constant on the cation and varying the anion results in a decrease in the surface tension for a smaller anion, e.g., from [PF₆]⁻ to [BF₄]⁻ or from [Br]⁻ to [Cl]⁻.²⁰ Hence, an increase from ethyl to butyl in the alkyl chain may be assumed to diminish the surface tension. Moreover, Franses et al.⁹⁸ performed surface tension measurements of aqueous sodium methyl sulfate as a function of its bulk concentration and presented a decrease in the surface tension at higher concentrations (> 20 mM). This may be used to further support the effect of an alkyl group on the lowering of the surface tension. Similar arguments are assumed to be valid for the methanesulfonate salts providing a thermodynamic justification for the CH₃ group of both anions present at the surface.

For the non-halide compounds, the earlier arguments indicate that the cation and anion share the surface. The question of whether the cation and anion adopt preferred orientations is now considered. In our earlier studies, SFG results suggested a model where the imidazolium ring lies nearly parallel to the surface with its butyl chain projecting toward the vapor phase.^{41,43}

A recent study on an [EMIM][Tf₂N] film using the combination of metastable impact electron spectroscopy (MEIS), X-ray photoelectron spectroscopy (XPS), and ultraviolet photoelectron spectroscopy (UPS) affirms that the surface layer consists of both a cation and an anion.³² Further, MEIS results suggest that the ethyl chain is also directed to the gas phase, which is in accordance with the SFG analysis. A simulation study on [BMIM]⁺ salts at the gas–liquid interface further confirms the suggested model, in which Del Popolo et al.⁴⁵ proposed that the butyl chain is indeed pointing toward the gas phase.

The orientation of the ring is believed to be parallel to the surface plane as suggested in the vibrational spectra. Given that SFG only probes molecules at the surface with polar ordering, the absence of the vibrational modes from C(2)–H, H–C(4)–C(5)–H, and N–CH₃ suggests that the most likely orientation for the ring is parallel to the surface plane. A recent study from

our laboratory presented a detailed analysis on the preferred orientation of the cation at the gas–liquid interface with a range of anions.⁴² Results indicate that ionic liquids based on the [BMIM]⁺ cation exhibit similar orientations regardless of the anion. The same orientation applies for both ionic liquids considered here. In addition, the present study has an advantage of having an alkyl group in the anion, which exhibits vibrational modes in the IR range (2000–4000 cm⁻¹) of our present SFG setup. Hence, crystallographic evidence in support of SFG data makes it feasible to determine the orientation and the location of the cation and anion.

Here, the suggested model for the orientation and location of the ions at the surface as determined by SFG spectroscopy is supported by the structures obtained from X-ray diffraction of the bulk solidified ionic liquid. Diffraction data showed crystal structures of both ionic liquids where the methyl groups of the cation and anion are projected in the same direction with the butyl chain orthogonal to the imidazolium ring, which is in agreement with the SFG results. Further, the butyl chain propagates in an *all-trans* conformation, which explains the absence of vibrational modes from the CH₂ groups in the SFG spectra. These modes are not allowed in SFG due to the local centrosymmetry of an *all-trans* chain conformation.⁵⁷

The tilt angle of the CH₃ group has also been determined from X-ray results. The C3 axis of the methyl group at the end of the butyl chain is positioned at approximately 37.8° and 42.0° with respect to the imidazolium ring normal for [BMIM][MS] and [BMIM][CH₃SO₃], respectively, while the methyl group of the methyl sulfate anion is tilted at around 48.9° and that of the methanesulfonate anion at 47.6° with respect to the normal of the imidazolium ring. In contrast to X-ray data, SFG results present a wider distribution of the average tilt angles for the C3 axis. The methyl group at the end of the butyl chain is determined to be near 53°, while that of the methyl sulfate is analyzed to be around 62°. Both angles were measured with respect to the surface normal. Given that the null angle for $\nu_{s(\text{CH}_3)}$ is similar for [BMIM]⁺ in all ionic liquids, then the [BMIM]⁺ cation for the methanesulfonate salt possesses a similar tilt angle. As mentioned earlier, the tilt angle for the methanesulfonate anion has not been analyzed since the null angle might be inaccurate due to the overlapping of peaks between $\nu_{s(\text{CH}_3-\text{CH}_3\text{SO}_3)}$ and $\nu_{\text{CH}_3-\text{FR}}$. The discrepancy in the measured tilt angles for the two techniques is interesting to note. Results from X-ray crystallography show smaller tilt angles compared to the SFG data. The difference might be due to the broad orientational distribution of the CH₃ groups at the interface for the liquid molecules, which suggests the more random nature of the vapor–liquid interface.

It is believed that the cation and anion are located adjacent to one another as evident in the X-ray results. In fact, the crystal structures of both compounds share similar features, even with different crystal packings. Assuming that a similar situation continues to the liquid state and to the surface, then a similar molecular arrangement can be expected at the surface. However, two other possible arrangements, where one of the ions is positioned either below or above the other, can be considered. For both arrangements, the CH₃ group from the butyl chain is particularly considered to be pointing upward as suggested from SFG and X-ray analyses. If on average the anion lies beneath the imidazolium ring, then the methyl group would be pointing downward in this positioning due to the presence of electrostatic interaction. Since this arrangement is inconsistent with the phase and X-ray analyses, this is the unlikely arrangement of the ions at the surface. On the other hand, if the anion is supposed to lie

above the ring with the CH₃ group upward, then it is consistent with the results where SFG spectra show vibrational modes from the anion. However, this arrangement would likely disrupt an *all-trans* conformation of the butyl chain, which may lead to some defects, and possibly shows the CH₂ modes in the SFG spectra. In addition, if this is the possible orientation, then the charged parts of the cation and anion would be closely associated with one another. In this situation, hydrogen bonding must be substantial between the oxygen atoms of the anion and the protons of the imidazolium ring, which is not the case as mentioned earlier. Surprisingly, for [BMIM][MS], no such interactions have been detected. Instead the anion is more associated with the methyl group of the ring than the charged part of it, as shown in Figure 9. Although the interaction between the proton of the C(2) atom and one of the oxygen atoms is present in [BMIM][CH₃SO₃], it is considered less significant. On the basis of the preceding arguments, it seems likely that the cation and anion at the gas–liquid interface are adjacent to one another, with the methyl sulfate and methanesulfonate anions closer to the methyl group attached to the nitrogen atoms, as supported by SFG and crystallographic evidence. This preferential positioning of the ions is surprising since previous studies showed that the anion is most likely associated with the most acidic proton of the imidazolium ring, C(2)H.

There are few experimental and simulation studies on the molecular composition and orientation at the surface of ionic liquids, but most of them employed imidazolium-based ionic liquids with fluorinated anions, e.g., [PF₆]⁻ and [BF₄]⁻, and others include [Tf₂N]⁻ and [NO₃]⁻ anions; no report has been made yet on the ionic liquids with an alkyl group on the anions. Conversely, different conclusions have been drawn from these investigations. As has been noted in the literature, DRS^{34–36} and SFG^{40–43} experiments have offered contradicting models of the surface orientation for the [BMIM]⁺ cation. DRS experiments suggest that the ring orientation is perpendicular to the surface with both nitrogens pointing upward and the butyl chain is parallel to the surface for [BMIM][PF₆], while it is pointing toward the bulk liquid for [BMIM][BF₄]. In addition, [PF₆]⁻ is claimed to be located over the C(2) atom of the cation. Deutsch et al.'s³⁷ results from the X-ray reflectivity technique on similar compounds are somewhat in agreement with the DRS data of Watson et al.,^{34–36} in which they also proposed two types of molecular arrangements at the surface, one with the chain parallel to the surface plane and the other with the chain normal to the surface. On the other hand, the conclusions drawn from the neutron reflectometry experiment regarding the orientation nearly coincide with our results, the ring being parallel to the surface plane but the tail groups tending to form a lamellar structure which is at least two tiers of alkyl chains.³⁸ However, the possible existence of surface layering was unable to be unambiguously demonstrated.

The proposed SFG model of the [BMIM]⁺ cation is further supported by the recent simulation studies of Balasubramanian et al.⁴⁶ on [BMIM][PF₆] and Voth et al.⁴⁴ on [EMIM][NO₃]. The results illustrate that, at the outermost layer of the surface, the probable orientation of the butyl chain is parallel to the surface normal, which is directed toward the gas phase. Hence, the surface possesses a certain amount of hydrophobicity due to the presence of an alkyl group.⁴⁶ Further, the imidazolium ring is found to be oriented parallel to the surface plane. Beneath this outermost layer is the dense region where the imidazolium ring is perpendicular to the surface plane. This observation coincides with the DRS findings of Watson et al.^{34–36} and the X-ray reflectivity of Deutsch et al.³⁷ In addition, conclusions

from reflectivity measurements reveal that the increase in the electron density at the interface, which is higher than that of the bulk, is consistent with the simulation analysis of Balasubramanian et al.⁴⁶ This enhancement is mainly due to the anion; therefore, it implies that both ions share the surface.

The simulation studies demonstrate that orientations observed experimentally are acceptable and the preferential ordering occurs at the first layer, with the SFG model showing it occurring at the outermost layer.

Conclusion

This work has shown the surface orientation of the ions 1-butyl-3-methylimidazolium cation and methyl sulfate and methanesulfonate anions using SFG spectroscopy along with the PNA measurements for a more accurate determination of the tilt angle of the methyl group. In addition, the phase of the methyl groups from the butyl chain, methyl sulfate, and methanesulfonate has also been determined using simulations which demonstrate that the methyl group is pointing away from the bulk liquid, implying that the butyl chain is also projecting away from the liquid phase. The structures of both ionic liquids have also been determined by X-ray crystallography. As a result of employing these two techniques, structural information on the solid state of the ionic liquid as well as the orientation and location of ions at the gas–liquid interface is obtained.

Acknowledgment. The support for this project was provided by the Robert A. Welch Foundation and the Petroleum Research Fund. The single-crystal X-ray diffraction instrument was provided by Professor J. Kochi of the Department of Chemistry at the University of Houston, Texas.

Supporting Information Available: Crystal structures of solidified ionic liquids used in this study and corresponding information provided as CIF files. This material is available free of charge via the Internet at <http://pubs.acs.org>.

References and Notes

- Dupont, J.; de Souza, R. F.; Suarez, P. A. *Z. Chem. Rev.* **2002**, *102*, 3667–3692.
- Mehner, C. P.; Cook, R. A.; Dispenziere, N. C.; Afeworki, M. *J. Am. Chem. Soc.* **2002**, *124*, 12932–12933.
- Welton, T. *Chem. Rev.* **1999**, *99*, 2071–2083.
- Wilkes, J. S.; Levisky, J. A.; Wilson, R. A.; Hussey, C. L. *Inorg. Chem.* **1982**, *21*, 1263–1264.
- Wasserscheid, P.; Keim, W. *Angew. Chem., Int. Ed.* **2000**, *39*, 3772–3789.
- Suarez, P. A. Z.; Einloft, S.; Dullius, J. E. L.; de Souza, R. F.; Dupont, J. *J. Chim. Phys. Phys.-Chim. Biol.* **1998**, *95*, 1626–1639.
- Huddleston, J. G.; Visser, A. E.; Reichert, W. M.; Willauer, H. D.; Broker, G. A.; Rogers, R. D. *Green Chem.* **2001**, *3*, 156–164.
- Hagiwara, R.; Ito, Y. *J. Fluorine Chem.* **2000**, *105*, 221–227.
- Bonhote, P.; Dias, A.; Papageorgiou, N.; Kalyanasundaram, K.; Gratzel, M. *Inorg. Chem.* **1996**, *35*, 1168–1178.
- Huddleston, J. G.; Willauer, H. D.; Swatloski, R. P.; Visser, A. E.; Rogers, R. D. *Chem. Commun.* **1998**, 1765–1766.
- Earle, M. J.; Seddon, K. R. *Pure Appl. Chem.* **2000**, *72*, 1391–1398.
- Seddon, K. R. *J. Chem. Technol. Biotechnol.* **1997**, *68*, 351–356.
- Armstrong, D. W.; He, L.; Liu, Y.-S. *Anal. Chem.* **1999**, *71*, 3873–3876.
- Blanchard, L. A.; Brennecke, J. F. *Ind. Eng. Chem. Res.* **2001**, *40*, 287–292.
- Holbrey, J. D.; Seddon, K. R. *Clean Prod. Processes* **1999**, *1*, 223–236.
- Quinn, B. M.; Ding, Z.; Moulton, R.; Bard, A. J. *Langmuir* **2002**, *18*, 1734–1742.
- Tokuda, H.; Hayamizu, K.; Ishii, K.; Susan, M.; Watanabe, M. *J. Phys. Chem. B* **2004**, *108*, 16593–16600.
- Tokuda, H.; Ishii, K.; Susan, M.; Tsuzuki, S.; Hayamizu, K.; Watanabe, M. *J. Phys. Chem. B* **2006**, *110*, 2833–2839.

- Fredlake, C. P.; Crosthwaite, J. M.; Hert, D. G.; Aki, S.; Brennecke, J. F. *J. Chem. Eng. Data* **2004**, *49*, 954–964.
- Law, G.; Watson, P. R. *Langmuir* **2001**, *17*, 6138–6141.
- Tokuda, H.; Hayamizu, K.; Ishii, K.; Susan, M.; Watanabe, M. *J. Phys. Chem. B* **2005**, *109*, 6103–6110.
- Anthony, J. L.; Maginn, E. J.; Brennecke, J. F. *J. Phys. Chem. B* **2002**, *106*, 7315–7320.
- Cadena, C.; Anthony, J. L.; Shah, J. K.; Morrow, T. I.; Brennecke, J. F.; Maginn, E. J. *J. Am. Chem. Soc.* **2004**, *126*, 5300–5308.
- Buzzeo, M. C.; Klymenko, O. V.; Wadhawan, J. D.; Hardacre, C.; Seddon, K. R.; Compton, R. G. *J. Phys. Chem. B* **2004**, *108*, 3947–3954.
- Camper, D.; Scovazzo, P.; Koval, C.; Noble, R. *Ind. Eng. Chem. Res.* **2004**, *43*, 3049–3054.
- Bowers, J.; Butts, C. P.; Martin, P. J.; Vergara-Gutierrez, M. C.; Heenan, R. K. *Langmuir* **2004**, *20*, 2191–2198.
- Halka, V.; Tsekov, R.; Freyland, W. *Phys. Chem. Chem. Phys.* **2005**, *7*, 2038–2043.
- Martino, W.; de la Mora, J. F.; Yoshida, Y.; Saito, G.; Wilkes, J. *Green Chem.* **2006**, *8*, 390–397.
- Visser, A. E.; Reichert, W. M.; Swatloski, R. P.; Willauer, H. D.; Huddleston, J. G.; Rogers, R. D. ACS Symposium Series 818; American Chemical Society: Washington, DC, 2002; pp 289–308.
- Sung, J.; Jeon, Y.; Kim, D.; Iwahashi, T.; Iimori, T.; Seki, K.; Ouchi, Y. *Chem. Phys. Lett.* **2005**, *406*, 495–500.
- Smith, E. F.; Garcia, I. J.; Briggs, D.; Licence, P. *Chem. Commun.* **2005**, 5633–5635.
- Hofft, O.; Bahr, S.; Himmerlich, M.; Krischok, S.; Schaefer, J. A.; Kemper, V. *Langmuir* **2006**.
- Fortunato, R.; Alfonso, C. A. M.; Benavente, J.; Rodriguez-Castellon, E.; Crespo, J. G. *J. Membr. Sci.* **2005**, *256*, 216–223.
- Gannon, T. J.; Law, G.; Watson, P. R. *Langmuir* **1999**, *15*, 8429–8434.
- Law, G.; Watson, P. R. *Chem. Phys. Lett.* **2001**, *345*, 1–4.
- Law, G.; Watson, P. R.; Carmichael, A. J.; Seddon, K. R. *Phys. Chem. Chem. Phys.* **2001**, *3*, 2879–2885.
- Sloutskin, E.; Ocko, B. M.; Tamam, I.; Kuzmenko, I.; Gog, T.; Deutsch, M. *J. Am. Chem. Soc.* **2005**, *127*, 7796–7804.
- Bowers, J.; Vergara-Gutierrez, M. C. *Langmuir* **2004**, *20*, 309–312.
- Iimori, T.; Iwahashi, T.; Ishii, H.; Seki, K.; Ouchi, Y.; Ozawa, R.; Hamaguchi, H.; Kim, D. *Chem. Phys. Lett.* **2004**, *389*, 321–326.
- Rivera-Rubero, S.; Baldelli, S. *J. Phys. Chem. B* **2006**, *110*, 15499–15505.
- Baldelli, S. *J. Phys. Chem. B* **2003**, *107*, 6148–6152.
- Rivera-Rubero, S.; Baldelli, S. *J. Phys. Chem. B* **2006**, *110*, 4756–4765.
- Rivera-Rubero, S.; Baldelli, S. *J. Am. Chem. Soc.* **2004**, *126*, 11788–11789.
- Yan, T.; Li, S.; Jiang, W.; Gao, X.; Xiang, B.; Voth, G. A. *J. Phys. Chem. B* **2006**, *110*, 1800–1806.
- Lynden-Bell, R. M.; Del Popolo, M. G. *Phys. Chem. Chem. Phys.* **2006**, *8*, 949–954.
- Bhargava, B. L.; Balasubramanian, S. *J. Am. Chem. Soc.* **2006**, *128*, 10073–10078.
- Del Popolo, M. G.; Lynden-Bell, R. M.; Kohanoff, J. *J. Phys. Chem. B* **2005**, *109*, 5895–5902.
- Lynden-Bell, R. M. *Mol. Phys.* **2003**, *101*, 2625–2633.
- Holbrey, J. D.; Reichert, W. M.; Swatloski, R. P.; Broker, G. A.; Pitner, W. R.; Seddon, K. R.; Rogers, R. D. *Green Chem.* **2002**, *4*, 407–413.
- Holbrey, J. D.; Seddon, K. R. *J. Chem. Soc., Dalton Trans.* **1999**, 2133–2139.
- Fuller, J.; Carlin, R. T.; De Long, H. C.; Haworth, D. *J. Chem. Soc., Chem. Commun.* **1994**, 299–300.
- Holbrey, J. D.; Reichert, W. M.; Nieuwenhuyzen, M.; Johnston, S.; Seddon, K. R.; Rogers, R. D. *Chem. Commun.* **2003**, 1636–1637.
- Billard, I.; Moutiers, G.; Labet, A.; El Azzi, A.; Gaillard, C.; Mariet, C.; Lutzenkirchen, K. *Inorg. Chem.* **2003**, *42*, 1726–1733.
- Dibrov, S. M.; Kochi, J. K. *Acta Crystallogr., Sect. C: Cryst. Struct. Commun.* **2006**, *C62*, o19–o21.
- Downard, A.; Earle, M. J.; Hardacre, C.; McMath, S. E. J.; Nieuwenhuyzen, M.; Teat, S. *J. Chem. Mater.* **2004**, *16*, 43–48.
- Gordon, C. M.; Holbrey, J. D.; Kennedy, A. R.; Seddon, K. R. *J. Mater. Chem.* **1998**, *8*, 2627–2636.
- Bain, C. D. *J. Chem. Soc., Faraday Trans.* **1995**, *91*, 1281–1296.
- Miranda, P. B.; Shen, Y. R. *J. Phys. Chem. B* **1999**, *103*, 3292–3307.
- Buck, M.; Himmelhaus, M. *J. Vac. Sci. Technol., A* **2001**, *19*, 2717–2736.
- Shultz, M.; Baldelli, S.; Schnitzer, C.; Simonelli, D. *J. Phys. Chem. B* **2002**, *106*, 5313–5324.
- Zhuang, X.; Miranda, P. B.; Kim, D.; Shen, Y. R. *Phys. Rev. B* **1999**, *59*, 12632–12640.

- (62) Fitchett, B. D.; Conboy, J. C. *J. Phys. Chem. B* **2004**, *108*, 20255–2–262.
- (63) Guyot-Sionnest, P.; Hunt, J. H.; Shen, Y. R. *Phys. Rev. Lett.* **1987**, *59*, 1597–1600.
- (64) Tyrode, E.; Johnson, C. M.; Baldelli, S.; Leygraf, C.; Rutland, M. W. *J. Phys. Chem. B* **2005**, *109*, 329–341.
- (65) Romero, C.; Baldelli, S. *J. Phys. Chem. B* **2006**, *110*, 6213–6223.
- (66) Lu, R.; Gan, W.; Wang, H.-F. *Chin. Sci. Bull.* **2003**, *48*, 2183–2187.
- (67) Wang, H.-F.; Gan, W.; Lu, R.; Rao, Y.; Wu, B.-H. *Int. Rev. Phys. Chem.* **2005**, *24*, 191.
- (68) Gan, W.; Wu, B.; Chen, H.; Guo, Y.; Wang, H.-F. *Chem. Phys. Lett.* **2005**, *406*, 467–473.
- (69) Chen, H.; Gan, W.; Wu, B.; Wu, D.; Zhang, Z.; Wang, H.-F. *Chem. Phys. Lett.* **2005**, *408*, 284–289.
- (70) Santos, C.; Baldelli, S. Manuscript in preparation.
- (71) Ren, R. X.; Robertson, A. PCT Patent WO/03/051894, 2003.
- (72) Bruker SMART version 5.630 Data Collection and SAINT-Plus version 6.28 Data Processing Software for the SMART System, Bruker Analytical X-ray Instruments, Inc., Madison, WI, 2003.
- (73) Sheldrick, G. M. SHELXTL version 6.12, Bruker Analytical X-ray Instruments, Inc., Madison, WI, 2003.
- (74) MacPhail, R. A.; Strauss, H. L.; Snyder, R. G.; Elliger, C. A. *J. Phys. Chem.* **1984**, *88*, 334.
- (75) Snyder, R. G. *J. Chem. Phys.* **1965**, *42*, 1744.
- (76) Lu, R.; Gan, W.; Wu, B.; Zhang, Z.; Guo, Y.; Wang, H.-F. *J. Phys. Chem. B* **2005**, *109*, 14118–14129.
- (77) Superfine, R.; Huang, J. Y.; Shen, Y. R. *Phys. Rev. Lett.* **1991**, *66*, 1066–1069.
- (78) Tuttolomondo, M. E.; Navarro, A.; Pena, T.; Varetto, E. L.; Altabef, A. *J. Phys. Chem. A* **2005**, *109*, 7946–7956.
- (79) Thompson, W. K. *Spectrochim. Acta* **1972**, *28A*, 1479–1484.
- (80) Capwell, R. J.; Rhee, K. H.; Seshadri, K. S. *Spectrochim. Acta* **1968**, *24A*, 955–958.
- (81) Allen, H. C.; Raymond, E. A.; Richmond, G. L. *J. Phys. Chem. A* **2001**, *105*, 1649–1655.
- (82) Carter, D. A.; Pemberton, J. E. *J. Raman Spectrosc.* **1997**, *28*, 939–946.
- (83) Superfine, R.; Huang, J. Y.; Shen, Y. R. *Chem. Phys. Lett.* **1990**, *172*, 303.
- (84) Superfine, R.; Huang, J. Y.; Shen, Y. R. *Opt. Lett.* **1990**, *15*, 1276.
- (85) Carmichael, A. J.; Hardacre, C.; Holbrey, J. D.; Seddon, K. R.; Nieuwenhuyzen, M. *Electrochemical Society Proceedings*; pp 209–221.
- (86) Martin, J. D. In *Ionic Liquids: Industrial Applications for Green Chemistry*; Rogers, R., Seddon, K. R., Eds.; American Chemical Society: Washington, DC, 2002.
- (87) Hardacre, C.; Holbrey, J. D.; McMath, S. E.; Bowron, D. T.; Soper, A. K. *J. Chem. Phys.* **2003**, *118*, 273–278.
- (88) Hardacre, C.; McMath, S. E.; Nieuwenhuyzen, M.; Bowron, D. T.; Soper, A. K. *J. Phys.: Condens. Matter* **2003**, *15*, S159–S166.
- (89) Bradley, A. E.; Hardacre, C.; Holbrey, J. D.; Johnston, S.; McMath, S. E. J.; Nieuwenhuyzen, M. *Chem. Mater.* **2002**, *14*, 629–635.
- (90) Holbrey, J. D.; Reichert, W. M.; Nieuwenhuyzen, M.; Sheppard, O.; Hardacre, C.; Rogers, R. D. *Chem. Commun.* **2003**, 476–477.
- (91) Bolte, M.; Griesinger, C.; Sakhaei, P. *Acta Crystallogr., Sect. E: Struct. Rep.* **2001**, *E57*, o458–o460.
- (92) Bowron, D. T.; Hardacre, C.; Holbrey, J. D.; McMath, S. E. J.; Nieuwenhuyzen, M.; Soper, A. K. ACS Symposium Series; American Chemical Society: Washington, DC, 2003; pp 151–161.
- (93) Adamson, A. W.; Gast, A. P. *Physical Chemistry of Surfaces*; 6th ed.; John Wiley & Sons, Inc.: New York, 1997.
- (94) Langmuir, I. *Phenomena, Atoms, and Molecules*; Philosophical Library, Inc.: New York, 1950.
- (95) Langmuir, I. *Chem. Metall. Eng.* **1916**, 468–470.
- (96) Langmuir, I. *J. Am. Chem. Soc.* **1916**, *38*, 2221–2295.
- (97) Yang, J.-Z.; Lu, X.-M.; Guic, J.-S.; Xua, W.-G. *Green Chem.* **2004**, *6*, 541–543.
- (98) Prosser, A. J.; Franses, E. I. *Langmuir* **2002**, *18*, 9234–9242.